



## Ultra-high efficient hydrodynamic cavitation enhanced oxidation of nitric oxide with chlorine dioxide

Liguo Song<sup>a,b,\*</sup>, Jingang Yang<sup>a</sup>, Shubo Yu<sup>a</sup>, Minyi Xu<sup>a</sup>, Yuanchuang Liang<sup>a</sup>, Xinxiang Pan<sup>a,b,\*</sup>, Li Yao<sup>a</sup>

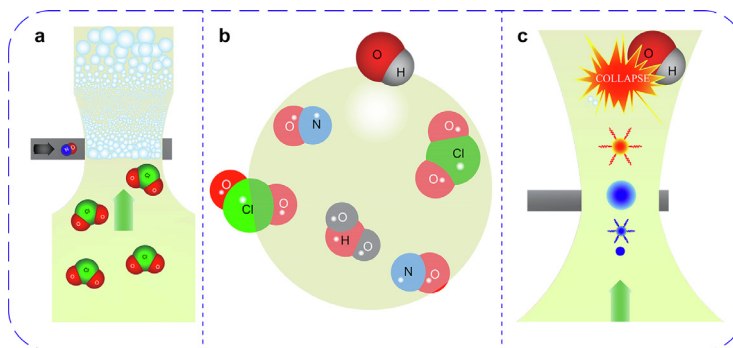
<sup>a</sup> Marine Engineering College, Dalian Maritime University, Dalian, Liaoning 116026, China

<sup>b</sup> Guangdong Ocean University, Zhanjiang, Guangdong 524088, China

### HIGHLIGHTS

- Hydrodynamic cavitation reactor is employed to remove NO in the exhaust gas.
- Hydrodynamic cavitation reactor expanded the gas-liquid contact area by more than 37.5 times.
- NO<sub>x</sub> removal rate was over 90% at even 1.0 mg/L ClO<sub>2</sub>.
- NO<sub>2</sub> concentration was very low during all experiments.

### GRAPHICAL ABSTRACT



### ARTICLE INFO

#### Keywords:

Hydrodynamic cavitation reactor  
Chlorine dioxide  
Wet denitration  
Marine air pollution

### ABSTRACT

Ships carry over 80% of the world's trade, and in the meantime, they cause severe air pollution. Nitrogen oxide (NO<sub>x</sub>) is one of the most difficult items to be treated among ship's air pollutants. In this paper, a novel treatment of gaseous pollutants based on hydrodynamic cavitation is proposed and systematically investigated. In comparison with the bubbling reactor, the hydrodynamic cavitation reactor (HC reactor) expanded the gas-liquid contact area by more than 37.5 times through generating microbubbles (about 0.50 mm) filled with the nitric oxide mixture (Gas-Filled-Bubbles). The small space inside the Gas-Filled-Bubble facilitated collisions of gas molecules, and thus accelerated the rate of gas phase chemical reactions. Furthermore, the collapse of cavitation bubbles (Cavities) may result in highly reactive free radicals and microjets, and the microjets helped to enhance gas-liquid mass transfer. The HC reactor had a longer duration for NO<sub>x</sub> removal rate over 90% than the bubbling reactor. When 1.0 mg/L chlorine dioxide (ClO<sub>2</sub>) solution was used, the duration for NO<sub>x</sub> removal rate over 90% was 100 s in the HC reactor, whereas in the bubbling reactor the duration was 0 s. Comparatively high ClO<sub>2</sub> concentration contributed to prolonged high NO<sub>x</sub> removal rate (≥ 90%) duration, however, the escape of ClO<sub>2</sub> would lead to more nitrogen dioxide (NO<sub>2</sub>) production, and poor ClO<sub>2</sub> utilization. The effects of the inlet and outlet pressures of the HC reactor on the denitrification effect were studied, and the cost-effectiveness of the proposed method was assessed. The results showed that the inlet pressure of 3.00 bar and the outlet pressure of 0.30 bar were reasonable options for HC reactor's denitration when both cost benefit and application conditions were taken into account.

\* Corresponding authors at: Marine Engineering College, Dalian Maritime University, Dalian, Liaoning 116026, China.

E-mail addresses: [songliguo@dmlu.edu.cn](mailto:songliguo@dmlu.edu.cn) (L. Song), [panxx@dmlu.edu.cn](mailto:panxx@dmlu.edu.cn) (X. Pan).

<https://doi.org/10.1016/j.cej.2019.05.094>

Received 18 January 2019; Received in revised form 13 May 2019; Accepted 15 May 2019

Available online 16 May 2019

1385-8947/ © 2019 Elsevier B.V. All rights reserved.

## 1. Introduction

The world commercial fleet on 1 January 2017 consisted of 93,161 vessels in total, with a combined tonnage of 1.86 billion dwt [1]. Ships carry over 80% of the world's trade [1–5], producing just 2–3% of its greenhouse gas emissions (GHG) [1–9]. Maritime transport is by far the most cost-effective way to transport goods around the world. However, ships cause severe air pollution problems, especially in coastal port cities and regions. Corbett et al. (2007) pointed out that particulate matter (PM) from ships caused approximately 60,000 deaths of cardiopulmonary and lung cancer annually, with most deaths occurring near coastlines in Europe, East Asia, and South Asia [10]. Sofiev et al. (2018) stated that before cleaner ship fuels was used, ship-related health impacted include about 400,000 premature deaths of lung cancer and cardiovascular disease and approximately 14 million childhood asthma cases annually [11]. According to the “2014 Hong Kong Emission Inventory Report”, 44% of SO<sub>x</sub>, 33% of NO<sub>x</sub>, 36% of respirable suspended particulates and 42% of fine suspended particulates in Hong Kong were discharged by ships, demonstrating that the air pollution of ships in port cities was severe. Shipping is a significant contributor to emissions of air pollutants [12,13] which needs to be focused now and future [14].

The Ship's NO<sub>x</sub> Emissions are getting more and more attention recently. Marine diesel engines, installed on ships which were built on or after January 1, 2016, and operating in NO<sub>x</sub> Emission Control Areas (NECA), shall comply with the Tier III NO<sub>x</sub> standard (3.4 g/kWh) which is 23.6% of Tier II standard (14.4 g/kWh). In order to meet the ship's fuel sulfur content standard (0.5% m/m) to be effective on January 1, 2020, a large number of ships have installed scrubber for exhaust desulfurization. The huge scrubber limits the installation of other large volume denitration equipment. Therefore, the method of simultaneous desulfurization and denitrification had caused concern in the industry.

NO accounts for more than 90% of the NO<sub>x</sub> in the exhaust gas [15–18], so the key to denitrification is to remove NO. NO<sub>x</sub> emission reduction techniques for engines include combustion control and post-combustion abatement technologies. For combustion control, many researchers in the shipping area focus on exhaust gas recirculation (EGR) [19–28] and alternative fuels (Liquefied Natural Gas (LNG), Hydrogen, Methanol) [29–31]. Energy efficiency, PM emissions, and carbon monoxide (CO) emissions are the most significant problems for EGR [29,32,33]. Exhaust gas temperature limits, PM emissions, flue gas cleanliness, installation space issues, and the impact of urea ammonia on crew life limit the application of selective catalytic reduction (SCR) [17,32–36]. The application of LNG can simultaneously reduce SO<sub>x</sub>, NO<sub>x</sub>, and PM, but storage, bunkering, and infrastructure related issues, as well as GHG emissions problems, cannot be resolved in the short term [29,32,37]. Based on the above reasons, there is no mature technology for ship denitration right now.

The convenient water environment of the ship provides a favorable condition for wet denitrification. Many scholars have researched simultaneous desulfurization and denitrification with the wet method. It has been found that the use of persulfate aqueous solutions, ClO<sub>2</sub>, NaClO<sub>2</sub>, and other oxidants could simultaneously remove SO<sub>x</sub> and NO<sub>x</sub> from the flue gas [38–40]. The use of an HC reactor for denitrification eliminates the need for a large scrubber. The installation of the grouping arrangement allows the HC reactor to be easily installed, which effectively reduces the volume and complexity of the ships' exhaust gas treatment device. Besides the use of HC reactor creates a vacuum at the flue gas inlet without causing an increase in the back pressure of the diesel engine. Since the HC reactor is insensitive to impurities in the exhaust gas, it is not easy to cause dirty plugging. Therefore, the HC reactor has a distinct advantage over traditional scrubbers.

The HC reactor can generate a large number of Gas-Filled-Bubbles. The Gas-Filled-Bubbles dramatically expanded the gas-liquid contact area and increased the chemical reaction rate (Fig. 1a). At the same

time, the oxidant molecules and water molecules diffused into the interior of the Gas-Filled-Bubbles undergone a gas phase reaction with the NO molecules (Fig. 1b). Moreover, the Gas-Filled-Bubbles were compressed and became smaller after being produced (Fig. 1a). The small space increased the collision chances of the molecules, which further strengthened the denitration effect.

Cavitation induces high pressure (10–500 MP) and high temperature (1000–15000 K) hot spots with unimaginable rapid heating rates (up to 10<sup>9</sup> K/s) in Cavities [41–46]. The extreme chemical reaction conditions in the Cavities are of great help in accelerating the chemical reactions [43,44,47]. The hydroxyl radical generated during the cavitation of water is a strong oxidizing substance, which also promotes the oxidation of NO (Fig. 1c). When Cavities collapse, the microjets generate turbulence and enhance the mass transfer of reactant [47]. Cavitation has been applied to biofuel refining [46,48–50], industrial wastewater treatment [47,48,51], and showed remarkable results.

To the best of our knowledge, cavitation has not been attempted to treat gas phase pollutants. In this study, we designed a gas treatment system wherein an HC reactor was applied. Comparative experiments on denitration of using the HC reactor and the bubbling reactor were carried out to verify the significant effect of hydrodynamic cavitation in denitrification. Then, the effects of ClO<sub>2</sub> concentration, the HC reactor inlet pressure and outlet pressure on denitration were studied. Moreover, the cost-benefit of the proposed method was assessed. We found that hydrodynamic cavitation significantly enhanced the NO<sub>x</sub> removal rate. The volume of the bubbles generated by the bubbling reactor was 53,420 times than that of the Gas-Filled-Bubbles. When 1.0 mg/L ClO<sub>2</sub> solution was used, the duration for NO<sub>x</sub> removal rate over 90% was 100 s for the HC reactor, whereas for the bubbling reactor the duration was 0 s. Comparatively high ClO<sub>2</sub> concentration contributed to prolonged high NO<sub>x</sub> removal rate duration, however, the escape of ClO<sub>2</sub> led to more NO<sub>2</sub> production, and poor ClO<sub>2</sub> utilization. The inlet pressure and outlet pressure of HC reactor were studied. Higher inlet pressure of HC reactor could promote the reaction rate but reduce the reaction time, while higher outlet pressure of HC reactor could reduce the reaction rate but prolong the reaction time. According to the cost and engine performance, the cavitation reactor inlet pressure of 3.00 bar and the outlet pressure of 0.30 bar were found to be reasonable choices in these experiments.

## 2. Results and discussion

### 2.1. Comparison of denitration effects between the HC reactor and the bubbling reactor.

#### 2.1.1. The HC reactor improved the gas-liquid contact area

To study the denitration effects of hydrodynamic cavitation, comparative experiments of using an HC reactor and a bubbling reactor were carried out (Fig. 2). Two sets of experiments were conducted under the same condition except for the reactor. The photograph of the Gas-Filled-Bubbles produced by the HC reactor during hydrodynamic cavitation denitration experiments showed that the HC reactor produced a massive amount of Gas-Filled-Bubbles in the tube during denitration experiment (Fig. 2a). At the bottom part of the tube, the diameter of Gas-Filled-Bubbles was about 0.62 mm. Even after experiencing the polymerization growth in subsequent pipelines, the Gas-Filled-Bubbles size was only about 4.06 mm in the first stage gas-liquid separator/bubbling reactor (Fig. 2b). Correspondingly, in the comparative experiments, it was found that the size of the bubbles in the first stage gas-liquid separator/bubbling reactor during bubbling denitration was about 23.19 mm (Fig. 2c). The average volume of the bubbling bubbles was about 53,420 times the volume of the Gas-Filled-Bubbles. Compared with bubbling denitrification, hydraulic cavitation denitrification greatly increased the gas-liquid contact area and promoted gas-liquid mixing.

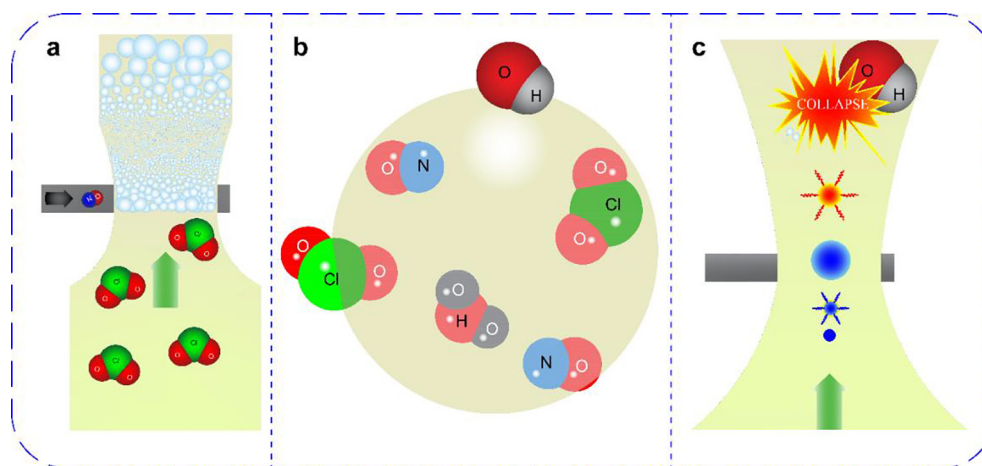


Fig. 1. Denitration mechanism of HC reactor using  $\text{ClO}_2$ . (a). Gas-Filled-Bubbles generated by HC reactor in  $\text{ClO}_2$  solution. (b). Distribution of molecules inside and outside a single Gas-Filled-Bubble. (c). Cavitation in HC reactor.

### 2.1.2. Effect of free radicals generated by hydrodynamic cavitation on the denitration

Water molecules can be pyrolyzed into  $\cdot\text{OH}$  and  $\cdot\text{H}$  radicals in the gas phase inside and in the interfacial region of the cavities from reaction Eq. (1) [52,53]



The  $\cdot\text{OH}$  will recombine to form  $\text{H}_2\text{O}_2$  in an aqueous phase from reaction Eq. (1) [53,54]



Only about 10% of free radicals may move into the bulk-liquid phase and react with the substrate [55].

$\text{NO}_x$  may react either in the gas phase of cavities or in the interfacial zone with free radicals, ultimately transforming to nitrous ( $\text{HNO}_2$ ) and nitric acids ( $\text{HNO}_3$ ) (Eqs. (3)–(7)) [56]



Kohno et al. studied the free radical generation pattern of water with different dissolved gas molecules ( $\text{O}_2/\text{N}_2/\text{H}_2/\text{Ar}/\text{Ne}/\text{He}$ ). They found that both  $\cdot\text{OH}$  and  $\cdot\text{H}$  were detected in  $\text{Ar}/\text{Ne}/\text{He}$  dissolved water, and the ratios of  $\cdot\text{H}$  and  $\cdot\text{OH}$  were near 2:1. One possible reason was that hydrated electron ( $e_{\text{aq}}^-$ ) increased the level of  $\cdot\text{H}$  from the reaction Eqs. (8) and (9) [57]



In the core of cavities, the concentration of electrons upon electric breakdown can be high enough and, thus, led to the formation of  $e_{\text{aq}}^-$  as well as increased the level of  $\cdot\text{H}$  according to the reaction  $\cdot\text{H} + \text{OH}^- \leftrightarrow \text{H}_2\text{O} + e_{\text{aq}}^-$ . However, Gutiérrez and Henglein reported that the pK value of this equilibrium is 9.8 [58]. In our study, with the pH ranging from 4.54 to 5.63, most of the  $\text{OH}^-$  would be protonated into  $\text{H}_2\text{O}$ , so that the yield of  $\cdot\text{H}$  was suppressed.

In addition,  $\cdot\text{H}$  is an extremely strong reducing species and may participate in the reaction Eqs. (10)–(15). Reaction Eq. (15) had been used to explain why the  $\cdot\text{OH}$  radical yield exceeds that of the  $\cdot\text{H}$  atom yield in the sonolysis of argon-saturated water [59].



Therefore,  $\cdot\text{H}$  should be less than  $\cdot\text{OH}$  in this study and affected little on the reaction of nitrogen oxides.

The results of pure water denitration using HC reactor were shown in Supplementary Fig. 1B. The apparent duration maintained  $\text{NO}_x$  removal rate higher than 90% was 35 s for pure water and then the removal rate drops sharply. If a large amount of highly reactive radicals ( $\cdot\text{OH}$ ,  $\cdot\text{H}$ ) produced participated in the chemical reaction with  $\text{NO}$  in the HC reactor, the removal rate would not drop quickly from 89.6% (40 s) to 76.7% (45 s) in 5 s as the experimental results showed. Pipeline design and testing methods should be responsible for the 35 s of higher removal rate duration for pure water denitration.

Furthermore, the collapse of the cavity is dimensionally dependent. Above 2–10  $\mu\text{m}$ , the bubbles do not collapse, below which free radicals are not generated [60]. The HC reactor induced liquid cavitation while inhaling the gas. A large number of Gas-Filled-Bubbles were generated by the shearing action of the high-velocity liquid on the gas. These Gas-Filled-Bubbles (0.50–1.50 mm) were much larger than cavities and would not collapse when compressed. The presence of Gas-Filled-Bubbles buffered the pressure change of the liquid in the HC reactor, which was not conducive to the formation of cavities.

Therefore, in this study, the high activity free radicals produced by cavitation had little effect on denitration. The main reason for improving the denitration effect of  $\text{ClO}_2$  in the HC reactor may be that the HC reactor effectively improved the gas-liquid mass transfer process.

### 2.1.3. The HC reactor enhanced the gas phase reaction

Due to lower pressure inside the Gas-Filled-Bubbles, the  $\text{ClO}_2$  molecule and the water molecule would volatilize into the Gas-Filled-Bubbles and react with  $\text{NO}$  in the gas phase. The initial diameter of the Gas-Filled-Bubbles was compressed and became smaller in the diffuser section of the HC reactor. This facilitated collision among gas molecules and could increase the reaction rate. As the amount of Gas-Filled-Bubbles generated by the HC reactor was huge, the reaction of  $\text{ClO}_2$  to oxidize  $\text{NO}$  in the gas phase could not be neglected.

### 2.1.4. Effect of the HC reactor on the denitration

From the results of the  $\text{NO}_x$  removal rate during hydrodynamic cavitation and bubbling denitration experiments, it was shown that the

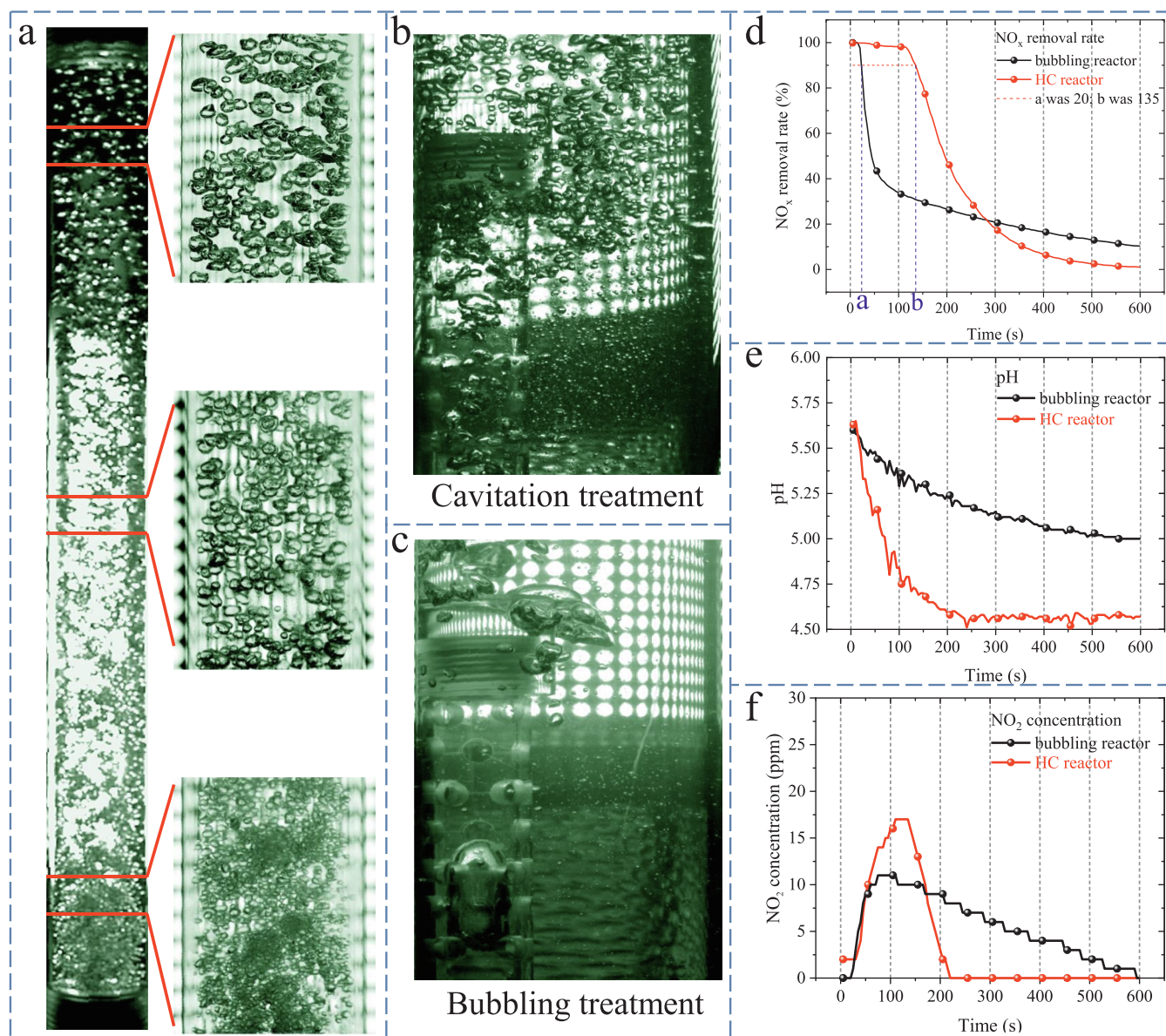


**Fig. 2.** Comparison of denitration effects between the HC reactor and the bubbling reactor. (Total liquid volume: 10.0 L; Gas flow: 1.4 L/min; NO concentration: 900 ppm; Liquid temperature: 20.0 °C; inlet pressure of the HC reactor: 3.00 bar; outlet pressure of the HC reactor: 0.30 bar; concentration of ClO<sub>2</sub> solution: 1.0 mg/L) (a). Photograph of the Gas-Filled-Bubbles just out of the HC reactor during hydrodynamic cavitation denitration experiment. (b). Photograph of the Gas-Filled-Bubbles produced in the first stage gas-liquid separator/bubbling reactor during hydrodynamic cavitation denitration experiment. (c). Photograph of the bubbles produced in the first stage gas-liquid separator/bubbling reactor during bubbling denitration experiment. (d). NO<sub>x</sub> removal rate during hydrodynamic cavitation and bubbling denitration experiments. (e). Changes in pH during hydrodynamic cavitation and bubbling denitrification experiments. (f). Changes in concentrations of NO<sub>2</sub> during hydrodynamic cavitation and bubbling denitrification experiments.

duration of the NO<sub>x</sub> removal rate over 90% was 135 s and 20 s for HC reactor and Bubbling reactor respectively (Fig. 2d). The 20-second NO<sub>x</sub> removal rate over 90% duration in the bubbling denitration experiment was due to experimental equipment and measurement methods (Supplementary Fig. 1A). In comparison with the blank experiment, the actual duration of the NO<sub>x</sub> removal rate over 90% was 100 s for hydrodynamic cavitation denitration experiment and 0 s for bubbling denitration experiment (Supplementary Fig. 1). For the hydrodynamic cavitation denitration, after 135 s of effective treatment, the NO<sub>x</sub> removal rate decreased sharply. At the 285th second, the NO<sub>x</sub> removal rate reduced to equal that of the bubbling denitration, and then continued to decrease below the bubbling denitration rate. In the final stage, the reason for the lower NO<sub>x</sub> removal rate of hydrodynamic cavitation denitrification was that most of the ClO<sub>2</sub> was consumed in the first 135 s, after which little ClO<sub>2</sub> remained. Conversely, the rate of

reaction for bubbling denitrification was lower, which allowed ClO<sub>2</sub> to oxidize NO over a more extended period slowly.

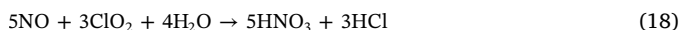
The pH also confirmed the higher denitration effect of hydrodynamic cavitation (Fig. 2e). In the hydrodynamic cavitation denitration experiment, the pH value rapidly decreased from 5.63 to 4.72 in the first 135 s, and then dropped slowly to 4.54 after 600 s reaction. The pH value reflected the absorption of the NO<sub>x</sub> to some extent. Eq. (18) showed that the more NO was oxidized, the more hydrochloric acid (HCl) and HNO<sub>3</sub> would be produced, and the lower pH would be reached. For the bubbling experiment, the pH value of the solution reduced slightly during the same period (from 5.61 to 5.00 in 600 s). The rapid drop in pH within 135 s indicated that HC reactor greatly increased the rate of chemical reaction, and the finally lower pH indicated a higher utilization of ClO<sub>2</sub> for hydrodynamic cavitation denitration.

The concentration of NO<sub>2</sub> showed interesting characteristics (Fig. 2f). During the hydrodynamic cavitation denitration experiment of ClO<sub>2</sub>, the concentration of NO<sub>2</sub> was found very low compared to other literature [61], and the pH was found to have little effect on the absorption of NO<sub>2</sub> (Fig. 2e–f). For the hydrodynamic cavitation denitration experiment, the concentration of NO<sub>2</sub> increased rapidly to 17 ppm (corresponding NO<sub>x</sub> removal rate was 97%, and corresponding pH was 4.77) and then decreased and remained at 0 (corresponding NO<sub>x</sub> removal rate was from 38.7% to 0%, and corresponding pH was about 4.55). The decreasing pH did not affect the concentration of NO<sub>2</sub>. While for the bubbling experiment, the concentration of NO<sub>2</sub> increased to about 11 ppm (corresponding NO<sub>x</sub> removal rate was 37.4%, and corresponding pH was 5.36) and decreased slowly to 0 ppm at 600 s (corresponding NO<sub>x</sub> removal rate was 10.3%, and corresponding pH was 5.0). The concentration of NO<sub>2</sub> reported in many literatures on wet denitrification was much higher than that in cavitation experiments, and as the pH decreased, the degree of absorption of NO<sub>2</sub> decreased [62–65]. The lower NO<sub>2</sub> concentration implied that hydrodynamic cavitation could promote the absorption of NO<sub>2</sub>.

The presence of NO<sub>2</sub> also indicated that the reaction of ClO<sub>2</sub> and NO was a step-by-step process. In the first step, ClO<sub>2</sub> oxidized NO to NO<sub>2</sub>, and in the second step, NO<sub>2</sub> was further oxidized to HNO<sub>3</sub> [66]:



The overall chemical reaction equation for the removal of NO<sub>x</sub> with ClO<sub>2</sub> was:



However, cavitation denitrification did not appear to be affected by pH and always had a high absorption rate of NO<sub>2</sub>. In the comparative experiment, the initial higher concentration of NO<sub>2</sub> in the cavitation experiment had two reasons. First, hydrodynamic cavitation enhanced the reaction of ClO<sub>2</sub> and NO. Since a large amount of NO<sub>2</sub> was produced instantaneously, the concentration of NO<sub>2</sub> was slightly increased despite the high absorption rate of NO<sub>2</sub>. Second, cavitation promoted the reaction of ClO<sub>2</sub> and NO<sub>x</sub>, but increased the escape as well, especially in the case of a high initial ClO<sub>2</sub> concentration. The evolved ClO<sub>2</sub> entrained some of the NO<sub>2</sub> to escape, resulting in a higher initial concentration of NO<sub>2</sub>.

Compared with other literatures, the hydrodynamic cavitation denitration experiment had achieved outstanding results. In this experiment, the NO<sub>x</sub> removal rate kept over 90% for about 100 s with 10.0 L of 1.0 mg/L ClO<sub>2</sub> solution. While Jin et al. used 1.11 mmol/min ClO<sub>2</sub> to oxidize NO (150 ppm–550 ppm), the NO<sub>x</sub> removal rate was about 70%. Moreover, no improvement in the NO<sub>x</sub> removal rate with the excess of ClO<sub>2</sub> [67]. In their experiment, the ClO<sub>2</sub> usage was 124.78 mg in 100 s, which was about 12.4 times the amount in the hydrodynamic cavitation denitration experiments. Han et al. used NaClO<sub>2</sub> solution in the scrubber reactor for denitration experiments. They used 20 mM NaClO<sub>2</sub> to absorb 1000 ppm NO. NO was almost absorbed, but about 300 ppm NO<sub>2</sub> was produced, the total denitration efficiency was about 70% [68]. In this experiment, the available chlorine concentration was about 1000 times the concentration in the hydrodynamic cavitation denitration experiments.

## 2.2. Effect of ClO<sub>2</sub> concentration on NO<sub>x</sub> removal effect.

Higher concentration of ClO<sub>2</sub> could promote the oxidation of NO, but it would cause an increase in the escape, which in turn affected the utilization of ClO<sub>2</sub>. To balance economics and efficiency, it is ideal for keeping the ClO<sub>2</sub> concentration as low as possible while maintaining high efficiency.

The impact of the concentration of ClO<sub>2</sub> was studied (Fig. 3a–f). As expected, with the increasing of ClO<sub>2</sub> concentration the denitration

effect was improved gradually (Fig. 3a). In other words, the higher the concentration of ClO<sub>2</sub> was, the longer the efficient treatment took (Fig. 3e). With the rapid consumption of ClO<sub>2</sub>, the NO removal rate gradually reduced to about 0% (Fig. 3a). Lower pH value meant higher denitration efficiency according to Eq. (18). When the concentration of ClO<sub>2</sub> was 0.0 mg/L, 0.2 mg/L, 0.4 mg/L, 0.6 mg/L, 0.8 mg/L, and 1.0 mg/L, the pH value of the solution respectively remained around 5.75, 5.21, 4.92, 4.78, 4.64 and 4.54 after 600 s (Fig. 3c). This further confirmed the effect of the concentration of ClO<sub>2</sub> on denitration.

The oxidation of NO by ClO<sub>2</sub> was a stepwise reaction, and NO<sub>2</sub> was an intermediate product and was further oxidized and then absorbed. A large amount of NO<sub>2</sub> produced in the initial stage of the reaction, resulting in incomplete absorption (Fig. 3b). However, the highest concentration of NO<sub>2</sub> in this experiment was only 17 ppm, so the NO removal rate and the NO<sub>x</sub> removal were almost the same (Fig. 3d).

The duration for the NO<sub>x</sub> removal rate over 90% was 135 s with 1.0 mg/L ClO<sub>2</sub> solution, while the duration with 0.0 mg/L ClO<sub>2</sub> solution was only 35 s, which might be the reason of the experiment design (Supplementary Fig. 1B). Therefore, the actual active duration of NO<sub>x</sub> removal rate over 90% was 100 s (Fig. 3e). The NO<sub>2</sub> concentration increased as ClO<sub>2</sub> concentration increased (Fig. 3b), which could be explained by the escaping property of ClO<sub>2</sub>. Higher ClO<sub>2</sub> concentration led to higher ClO<sub>2</sub> escape rate. The escape of ClO<sub>2</sub> carried NO<sub>2</sub>, resulting in a higher concentration of NO<sub>2</sub>. In order to make the ClO<sub>2</sub> escape effect more obvious, 30.0 mg/L ClO<sub>2</sub> was used to react with NO in the HC reactor. The results showed that NO maintained 100% removal rate in 65 min, and the highest NO<sub>2</sub> concentration was up to 128 ppm (Fig. 3f) which was much higher than 17 ppm by using 1.0 mg/L ClO<sub>2</sub> to denitration in the HC reactor. In the HC reactor, NO reacted from reactions Eqs. (16) and (17). Due to the excess of ClO<sub>2</sub> in the solution, the reaction rate of reaction Eq. (17) was mainly affected by the concentration of NO<sub>2</sub>. When 1.0 mg/L ClO<sub>2</sub> was used, the NO removal rate kept 100% for 100 s. This indicated that the 1.0 mg/L ClO<sub>2</sub> concentration had met the requirements of the chemical reaction Eq. (16). Increasing the concentration of ClO<sub>2</sub> could not make the reaction Eq. (16) faster and could not produce more NO<sub>2</sub>. Conversely, as the concentration of ClO<sub>2</sub> increased, the escape of ClO<sub>2</sub> gas increased. Hultén oxidized NO with ClO<sub>2</sub> gas in the first stage of a multi-component flue gas scrubber to produce NO<sub>2</sub>, which indicated that the reaction of ClO<sub>2</sub> and NO<sub>2</sub> was inactive in the gaseous state [39]. The escape of ClO<sub>2</sub> may act as an air flotation, causing NO<sub>2</sub> to escape. In the experiment, in order to protect the flue gas analyzer, a gas washing bottle was installed in front of the flue gas analyzer. When the concentration of ClO<sub>2</sub> increased, the yellow-green deionized water turned darker in the gas washing bottle, which also proved the escape of ClO<sub>2</sub>.

When ClO<sub>2</sub> concentration was 1.0 mg/L, the maximum concentration of NO<sub>2</sub> was 17 ppm, while ClO<sub>2</sub> concentration was 0.2 mg/L, there was no NO<sub>2</sub> detected. In order to reduce the production of NO<sub>2</sub> and the escape of ClO<sub>2</sub>, the lowest possible concentration of ClO<sub>2</sub> was the best choice under the premise of ensuring an efficient removal rate.

## 2.3. Effect of inlet pressure of the HC reactor on NO<sub>x</sub> removal rate.

The impact of the inlet pressure of the HC reactor on denitration was investigated (Fig. 4). The Gas-Filled-Bubbles became smaller as the inlet pressure increased. The Gas-Filled-Bubbles diameter was about 1.44 mm with 1.00 bar inlet pressure of the HC reactor, while it was 0.52 mm at 5.00 bar inlet pressure of the HC reactor. The Gas-Filled-Bubbles volume and the total gas-liquid contact area at 1.00 bar were about 20 times and 0.36 times the amount of their equivalents at 5.00 bar respectively (Fig. 4a). Higher inlet pressure promoted the gas-liquid mixing and increased the gas-liquid contact area. Therefore, the speed of the chemical reaction would increase with the increase of the inlet pressure for a certain period. As the inlet pressure increased, both the liquid flow rate and the volume of the ClO<sub>2</sub> solution flowing per unit time would increase. Accordingly, the liquid-gas ratio would

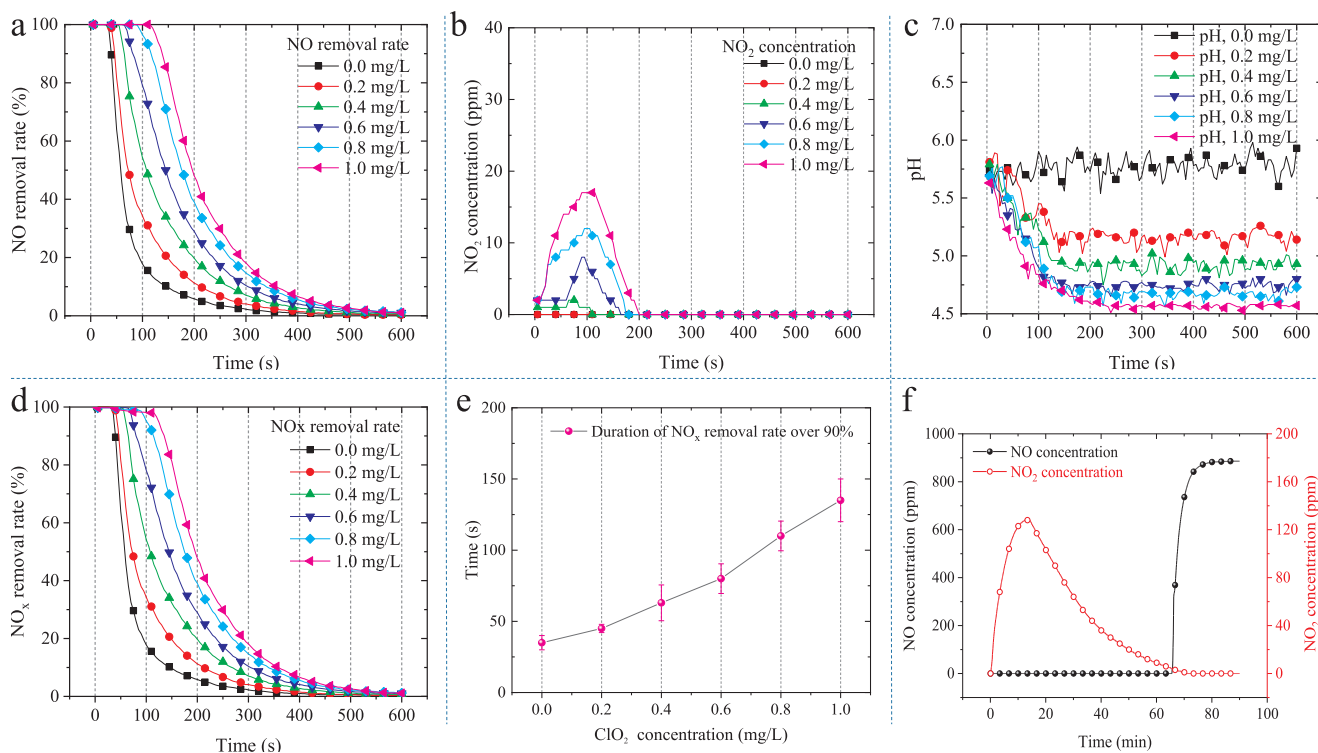


**Fig. 3.** The impact of the  $\text{ClO}_2$  concentration on denitration in the HC reactor. (Total liquid volume: 10.0 L; Gas flow: 1.4 L/min; NO concentration: 900 ppm; Liquid temperature: 20.0 °C; inlet pressure before HC reactor: 3.00 bar; outlet pressure after the HC reactor: 0.30 bar;  $\text{ClO}_2$  solution: 0.0 mg/L, 0.2 mg/L, 0.4 mg/L, 0.6 mg/L, 0.8 mg/L, 1.0 mg/L, 30.0 mg/L) (a). NO removal rate versus time at different concentrations of  $\text{ClO}_2$ . (b). The  $\text{NO}_2$  concentration versus time at different  $\text{ClO}_2$  concentrations. (c). pH of the solution versus time at different  $\text{ClO}_2$  concentrations. (d). The  $\text{NO}_x$  removal rate versus time at different  $\text{ClO}_2$  concentrations. (e). The durations of  $\text{NO}_x$  removal rate higher than 90% versus different  $\text{ClO}_2$  concentrations. (f). The NO and  $\text{NO}_2$  concentrations versus time for using 30.0 mg/L  $\text{ClO}_2$  to denitration.

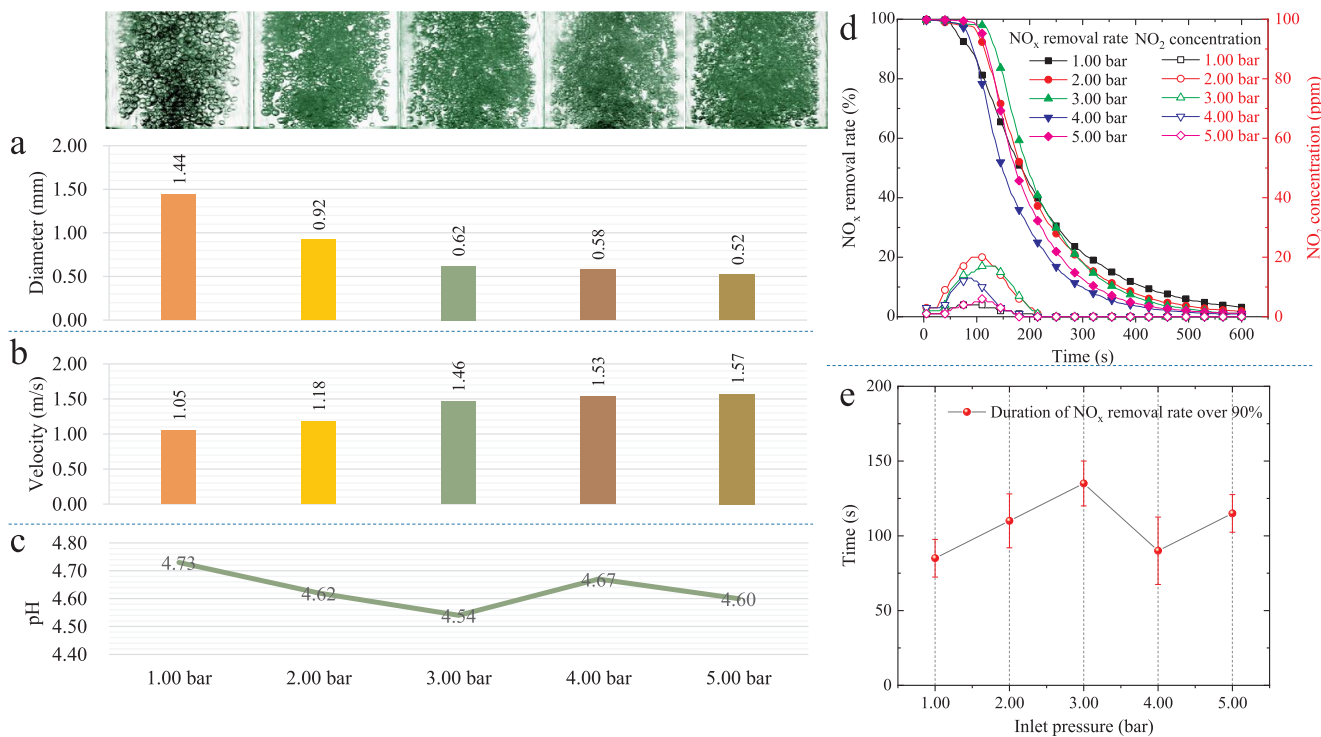


**Fig. 4.** The impact of the inlet pressures of HC reactor. ( $\text{ClO}_2$  solution: 1.0 mg/L; Total liquid volume: 10.0 L; Gas flow: 1.4 L/min; NO concentration: 900 ppm; Liquid temperature: 20.0 °C; outlet pressure after the HC reactor: 0.30 bar; inlet pressure before HC reactor: 1.00 bar, 2.00 bar, 3.00 bar, 4.00 bar, 5.00 bar) (a). Bubble diameter versus inlet pressures. (b). Bubble velocity versus inlet pressures. (c). pH values versus inlet pressures. (d).  $\text{NO}_x$  removal rate and  $\text{NO}_2$  concentration versus reaction time. (e). The duration of the  $\text{NO}_x$  removal rate over 90% versus inlet pressures.

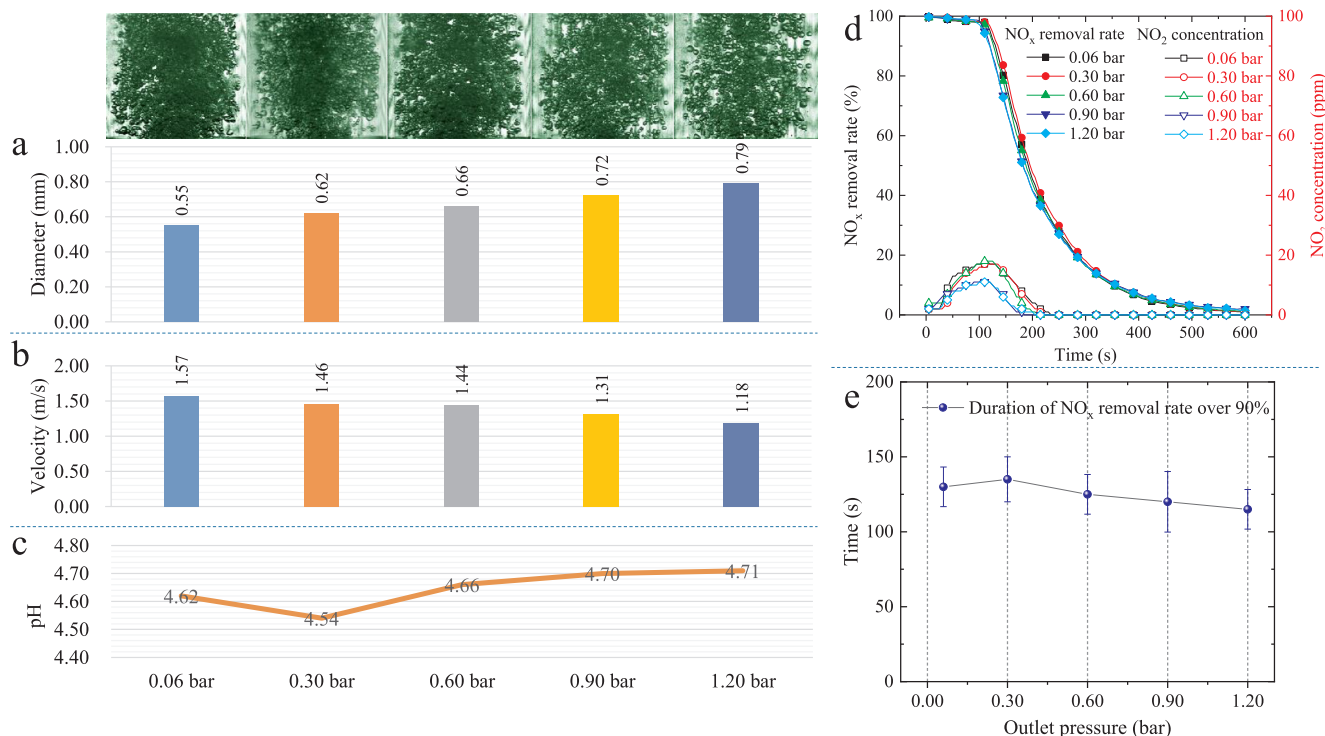


**Fig. 5.** The impact of the outlet pressures of HC reactor. (ClO<sub>2</sub> solution: 1.0 mg/L; Total liquid volume: 10.0 L; Gas flow: 1.4 L/min; NO concentration: 900 ppm; Liquid temperature: 20.0 °C; inlet pressure of the HC reactor: 3.00 bar; outlet pressure after HC reactor: 0.06 bar, 0.30 bar, 0.60 bar, 0.90 bar, 1.20 bar) (a). Bubble diameter versus outlet pressures. (b). Bubble velocity versus outlet pressures. (c). pH values versus outlet pressure. (d). NO<sub>x</sub> removal rate and NO<sub>2</sub> concentration versus reaction time. (e). The duration of the NO<sub>x</sub> removal rate over 90% versus outlet pressures.

increase, which also increased the chance of contact between NO molecular and ClO<sub>2</sub> molecular, thereby increasing the rate of chemical reactions. Higher inlet pressures could promote chemical reaction rate, but it also induced an increased liquid velocity that led to a reduction in overall chemical reaction time. As the inlet pressure increased from 1.00 bar to 5.00 bar, the bubble velocity increased from 1.05 m/s to 1.57 m/s (Fig. 4b). Gas-liquid contact time would decrease due to the increased inlet pressure. The change in the NO<sub>x</sub> removal rate reflected the competitive effect of increased reaction rate and reduced reaction time due to inlet pressure.

In addition to affecting the chemical reaction rate and total reaction time, the inlet pressure also had an effect on cavitation intensity in the experimental process. Cavitation number ( $C_v$ ) is a dimensionless parameter that represents the intensity of cavitation, defined as formula (19) [69],

$$C_v = \frac{p_2 - p_v}{1/2\rho V_{th}^2} \quad (19)$$

where  $p_2$  is the outlet pressure downstream of the venturi,  $p_v$  is the vapor pressure of the liquid at saturation temperatures, and  $V_{th}$  is the velocity of the liquid at the venturi throat and  $\rho$  is the liquid density.

The smaller Cavitation number is, the higher the cavitation intensity becomes. As discussed above, inlet pressure affected the liquid flow and the velocity of the liquid in the HC reactor.  $V_{th}$  would increase as inlet pressure increasing but not in a liner. Kumar et al. found that the cavitation number decreased as the inlet pressure increased, but became stable as the inlet pressure increased further [70]. The collapse of the Cavities produced strong microjets, which would enhance gas-liquid disturbances and promote gas-liquid mixing. Meanwhile, more hydroxyl radicals might be produced by a higher intensity of cavitation, which was also beneficial for the chemical reaction of denitrification [41–46].

On the other hand, similar to Cavities, the Gas-Filled-Bubbles experienced a rapid adiabatic compression process. The initial Gas-Filled-

Bubbles' pressure was equal to the minimum pressure caused by the cavitation reactor at the throat, and it was closely relating to the HC reactor's inlet pressure. The bigger the inlet pressure was, the lower the initial pressure of the Gas-Filled-Bubbles was. Since the outlet pressure was constant, as the inlet pressure of the HC reactor increased, the compression rate and compression speed of the Gas-Filled-Bubbles increased, resulting in a higher temperature in Gas-Filled-Bubbles. As the reaction of ClO<sub>2</sub> and NO is an exothermic reaction, a higher temperature will inhibit the rate of the reaction.

The overall effect of the inlet pressure on the denitrification effect was studied (Fig. 4d–e). The longest duration that maintained a NO<sub>x</sub> removal rate over 90% was 135 s, and the corresponding inlet pressure was 3.00 bar. Inlet pressures at 1.00 bar and 4.00 bar showed poor denitrification effect – the duration of NO<sub>x</sub> removal rate over 90% was 80 s and 90 s respectively. As the inlet pressure increased from 1.00 bar to 5.00 bar, the denitrification effect first increased and then decreased, and slowly increased again after 4.00 bar. Higher inlet pressures may have better denitrification effect than 3.00 bar but would result in increased energy consumption and tighter piping and equipment requirements, which were not suitable for practical applications.

During the experiment, the pH was measured continuously and used to support the experimental results. The initial pH value of the ClO<sub>2</sub> solution in this series of reactions was about 5.63, which was 4.73, 4.62, 4.54, 4.67 and 4.60 respectively, after 600 s of reaction (Fig. 4c). When the inlet pressure of the HC reactor was 3.00 bar, the pH of the solution was the lowest after 600 s of the experiment. Therefore, 3.00 bar was the optimum inlet pressure for hydrodynamic cavitation denitrification by use of ClO<sub>2</sub> in the range of 1.00 bar to 5.00 bar.

The trend of NO<sub>2</sub> concentration was basically proportional to the NO<sub>x</sub> removal rate. Within 220 s, the NO<sub>2</sub> concentration rose to 20 ppm and then dropped to 0 ppm (Fig. 4d). The low concentration of NO<sub>2</sub> demonstrated the high NO<sub>2</sub> absorption ability of the HC reactor. Since the oxidation rate of NO was higher than the absorption rate of NO<sub>2</sub>, despite the HC reactor's strong NO<sub>2</sub> absorption capacity, the higher

amount of NO<sub>2</sub> that was produced instantaneously led to higher NO<sub>2</sub> emissions.

#### 2.4. Effect of outlet pressure of the HC reactor on NO<sub>x</sub> removal effect

Similar to the inlet pressure of the HC reactor, the outlet pressure also affected the diameter and velocity of the Gas-Filled-Bubbles. The outlet pressure seriously affected the suction pressure of gas mixtures, so the outlet pressure changed little in the experiments. Fig. 5 showed the effect of outlet pressure on denitrification by use of the HC reactor. As the outlet pressure increased, the diameter of the Gas-Filled-Bubbles became larger (Fig. 5a). The Gas-Filled-Bubbles volume at the outlet pressure of 1.20 bar was approximately 2.9 times the volume of 0.06 bar. The Gas-Filled-Bubbles velocity decreased from 1.57 m/s to 1.18 m/s as the outlet pressure increased from 0.06 bar to 1.20 bar (Fig. 5b).

The results of the denitrification experiment at different outlet pressures were studied (Fig. 5d–e). The best experimental results were found at an outlet pressure of 0.30 bar, at which the NO<sub>x</sub> removal rate over 90% was 130 s. When the outlet pressure deviated from 0.30 bar, the duration of the NO<sub>x</sub> removal rate over 90% was shorter than the duration with 0.30 bar outlet pressure. The relationship of pH with outlet pressure also reflected the final experimental results (Fig. 5c). When the outlet pressure was 0.30 bar, the pH was the lowest, indicating that the optimum denitrification effect was achieved at the outlet pressure of 0.30 bar.

#### 2.5. Composition analysis of the reaction solution

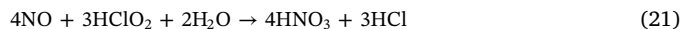
To understand the mechanism of NO removal in the HC reactor, the composition of the solution after the reaction was analyzed by ion chromatography. The ion chromatogram showed that the dominant ions in the solution after 600 s of reaction were chloride ion (Cl<sup>-</sup>), nitrite ion (NO<sub>2</sub><sup>-</sup>), chlorate ion (ClO<sub>3</sub><sup>-</sup>) and nitrate ion (NO<sub>3</sub><sup>-</sup>) (Fig. 6 and Supplementary Table S1). Among them, Cl<sup>-</sup> (0.335 mg/L) and NO<sub>3</sub><sup>-</sup> (0.479 mg/L) accounted for the majority.

The fact that the Cl<sup>-</sup> and NO<sub>3</sub><sup>-</sup> were predominant in the sample indicated that the oxidation of NO in the solution by ClO<sub>2</sub> occurs mainly through the process of Eqs. (16)–(18). ClO<sub>2</sub> is easily soluble in water but not easily hydrolyzed, and its solubility is ten times that of chlorine [71]. Most of the ClO<sub>2</sub> in the ClO<sub>2</sub> solution existed in a dissolved gas state, but a small amount of ClO<sub>2</sub> still disproportionated in water to form hypochlorous acid (HClO<sub>3</sub>) and chlorous acid (HClO<sub>2</sub>). The

reaction equation was as follows:



The HClO<sub>2</sub> had strong oxidizing properties in acid condition and was highly reactive with NO. The reaction equation was as follows:



Chlorite ion (ClO<sub>2</sub><sup>-</sup>) had a weak ability to work as an oxidizer in an alkaline solution but had a strong oxidative ability in an acidic medium [62]. Deshwal studied the removal of NO<sub>x</sub> from simulated flue gas using an acidic NaClO<sub>2</sub> solution. They found almost 100% oxidation of NO occurred at a pH ≤ 3.5, but at pH = 5, the oxidation rate of NO was only about 50%, while the NO<sub>x</sub> removal rate was about 20% [63]. Chien studied the use of NaClO<sub>2</sub> solution to remove SO<sub>2</sub> and NO from flue gas. They found that when the initial pH of the reaction solution was 5, the individual NO<sub>x</sub> removal rate was less than 10% (NaClO<sub>2</sub>/(SO<sub>2</sub> + NO) Ratio = 1.0) [16]. Horvath studied the detailed mechanism of the chlorite-tetrathionate reaction and found the pH dependence of the tetrathionate-chlorite reaction indicating a second-order dependence of H<sup>+</sup> on the reaction rate. In a slightly acidic condition (around pH = 5.35) the reaction proceeds relatively slowly [72,73]. Therefore the ClO<sub>2</sub><sup>-</sup> was not so reactive around pH = 5. Since the pH range of this experiment was 4.54 to 5.63, ClO<sub>2</sub><sup>-</sup> ions must be present in the solution after the reaction. In order to confirm the presence of ClO<sub>2</sub><sup>-</sup>, a spectrophotometer experiment was conducted, and the results were shown in (Supplementary Table S2). For the presence of NO<sub>2</sub><sup>-</sup>, the possible reason was that a small amount of NO<sub>2</sub> reacted directly with water to form HNO<sub>2</sub> and HNO<sub>3</sub>. The chemical equation was as follows:



#### 2.6. Energy balance calculation of the experiment.

In the experiment of denitrification by use of the HC reactor, the cost mainly included the cost of energy consumption, the cost of ClO<sub>2</sub>, and the cost of water. Considering the actual situation of the ship, we would not discuss the cost of water here.

##### 2.6.1. The energy balance calculation of the experiment

The energy consumption of this experiment could be calculated directly from the electrical energy consumed by the pump. However, since the experimental device was provided with a bypass line, the overall energy consumption was affected. For accurate calculations, we only calculated the energy consumed by the HC reactor.

The ClO<sub>2</sub> solution flowed into the HC reactor through section 1 and flowed out of the HC reactor through section 2 (Fig. 7). The HC reactor had a throttling consumption of the energy of the liquid. Since 99.9% of the gas inhaled by the HC reactor was water-insoluble argon and was mixed with the liquid in the form of tiny uniform bubbles, the liquid flowing out of the HC reactor could be assumed to be a low-density liquid.

According to the Bernoulli equation, the energy at Section 1 and Section 2 should satisfy the formula (23)

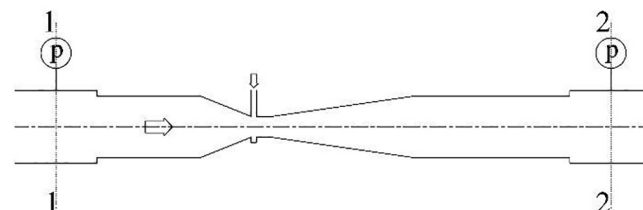


Fig. 7. HC reactor and the connecting pipelines.

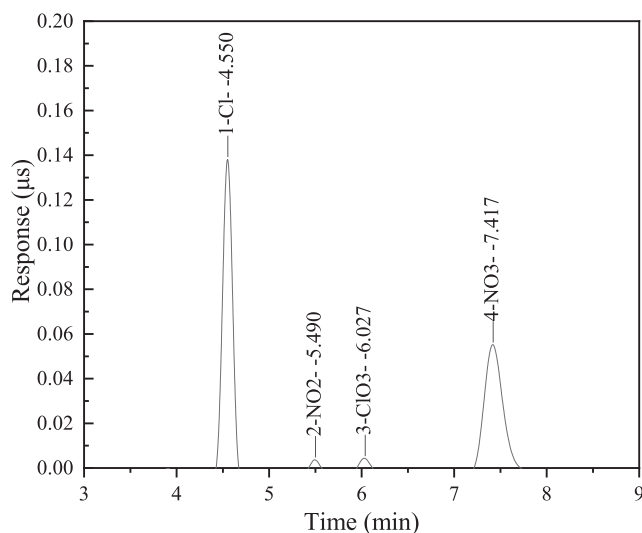


Fig. 6. Ion chromatogram of 1.0 mg/L ClO<sub>2</sub> solution after 600 s of NO removal in HC reactor.

$$\frac{v_1^2}{2g} + \rho_1 g h_1 + \frac{p_1}{\rho_1 g} = \frac{v_2^2}{2g} + \rho_2 g h_2 + \frac{p_2}{\rho_2 g} + \sum h \quad (23)$$

where

- $v_1$  was the liquid flow velocity at section 1, (m/s)
- $\rho_1$  was the density of the liquid before the HC reactor, (kg/m<sup>3</sup>)
- $p_1$  was the inlet pressure of the HC reactor, gauge pressure, (kPa)
- $h_1, h_2$  was the height of the liquid above the reference plane, (m)
- $v_2$  was the liquid flow velocity at section 1, (m/s)
- $\rho_2$  was the density of the liquid after the HC reactor, (kg/m<sup>3</sup>)
- $p_2$  was the outlet pressure of the HC reactor, gauge pressure, (kPa)
- $\sum h$  was the energy loss per second, (kJ)
- $g$  was the gravity acceleration, (m/s<sup>2</sup>)

The velocity of the liquid at section 1 could be calculated by the formula (24)

$$v_1 = \frac{Q_1}{3600 * \pi r_1^2} \quad (24)$$

where

- $Q_1$  was the liquid flow before HC reactor (m<sup>3</sup>/h)
- $r_1$  was the radius at section 1 (0.007 m)

Due to the inhalation of the gas, the volume of the liquid increased as it flowed through Section 2. The liquid flow through Section 2  $Q_2$  could be calculated by the formula (25)

$$Q_2 = \left( Q_1 + \frac{Q_{\text{gasinliquid}} * 10^{-3}}{3600} \right) \quad (25)$$

Since the gas was compressed by the liquid after being inhaled by the HC reactor, according to the ideal gas law, the flow of the gas in the liquid can be calculated by the formula (26)

$$Q_{\text{gasinliquid}} = \frac{P_{\text{atm}} * T_{\text{liquid}}}{(p_2 + P_{\text{atm}}) * T_0} * Q_g \quad (26)$$

where

- $Q_{\text{gasinliquid}}$  was the flow of compressed gas in the liquid, (L/h)
- $Q_g$  was the flow gas being inhaled in standard condition, (2.3 × 10<sup>-2</sup> L/h, 1.4 L/min)
- $P_{\text{atm}}$  was the standard atmospheric pressure (absolute pressure, 100 kPa)
- $T_{\text{liquid}}$  was the temperature of the liquid, (293.15 K)
- $T_0$  was 273.15 K

For different outlet pressure of the HC reactor,  $Q_{\text{gasinliquid}}$  was listed

**Table 1**  
The cost-benefit calculation of the experiment.

Gauge pressure			Liquid flow, $Q_1$	$Q_{\text{gasinliquid}}$	The effective duration, T	$\text{Cost}_E$	$\text{Cost}_C$	Cost
inlet	outlet	suction				84 m <sup>3</sup> /h, NO 900 ppm, 1.0 mg/LClO <sub>2</sub>		
(kPa)			(m <sup>3</sup> /h)	(L/h)	(s)	(CNY/day)		
100	30	13	0.24	6.46 × 10 <sup>-2</sup>	85	151	635	786
200	30	-16	0.36	6.46 × 10 <sup>-2</sup>	110	402	491	893
300	30	-35	0.45	6.46 × 10 <sup>-2</sup>	135	650	400	1050
400	30	-46	0.52	6.46 × 10 <sup>-2</sup>	90	896	600	1496
500	30	-51	0.57	6.46 × 10 <sup>-2</sup>	115	1142	470	1612
300	6	-47	0.46	7.93 × 10 <sup>-2</sup>	130	717	415	1133
300	30	-35	0.45	6.46 × 10 <sup>-2</sup>	135	650	400	1050
300	60	-17	0.44	5.25 × 10 <sup>-2</sup>	125	569	432	1001
300	90	1	0.43	4.42 × 10 <sup>-2</sup>	120	490	450	940
300	120	18	0.42	3.82 × 10 <sup>-2</sup>	115	412	470	882

in Table 1.

The velocity of the liquid at Section 2 could be calculated by the formula (27)

$$v_2 = \frac{Q_2}{3600 * \pi r_2^2} \quad (27)$$

where

$r_2$  was the radius at section 2 (0.007 m)

$$\rho_2 = \frac{Q_1}{Q_2} * \rho_1 \quad (28)$$

Taking the plane of the center line of the HC reactor as the reference plane, the energy consumption of the HC reactor per second can be expressed by the formula (29)

$$\sum h = \frac{Q_1^2 - Q_2^2}{2 * 3600^2 * \pi^2 r_1^2 r_2^2 g} + \frac{p_1}{\rho_1 g} - \frac{p_2}{\rho_2 g} \quad (29)$$

Since the experimental gas flow rate was only 1.4 L/min, in order to make the energy consumption result more intuitive and closer to reality, in the energy balance calculation, we assumed that 1000 HC reactors were connected in parallel and that the electricity price was 1 CNY/kWh. The 1-day electricity fee ( $\text{Cost}_E$ ) listed in Table 1 can be calculated using formula (30).

$$\text{Cost}_E = 24 * 1000 * 3600 * \frac{\sum h}{3600} \quad (30)$$

### 2.6.2. The cost of ClO<sub>2</sub>

In order to meet IMO's NO<sub>x</sub> emission standards, the NO<sub>x</sub> removal rate had to reach approximately 80%. In the hydrodynamic cavitation denitration experiment, when the NO<sub>x</sub> removal rate was reduced to 90%, the rate of decrease became faster, which was considered to be an indication of ClO<sub>2</sub> depletion. Therefore, the duration in which the NO<sub>x</sub> removal rate over 90% was defined as the effective denitration time T. T was summarized in Table 1 under different conditions. Since 10.0 L of 1.0 mg/L ClO<sub>2</sub> solution was used in the experiment, the mass of ClO<sub>2</sub> consumed in T was 10 mg. For different experimental conditions, the mass of ClO<sub>2</sub> consumed per second can be expressed by formula (31)

$$m_{\text{ClO}_2} = \frac{M_{\text{ClO}_2}}{T} \quad (31)$$

where

- $M_{\text{ClO}_2}$  was the mass of ClO<sub>2</sub> consumed in T, (1.0 × 10<sup>-5</sup> kg)
- $m_{\text{ClO}_2}$  was the mass of chlorine dioxide consumed in one second, (kg)
- T was the duration of NO<sub>x</sub> removal rate over 90%, (s)

Based on the same considerations of calculating energy

consumption, a 1000-fold flow of NO gas (84 m<sup>3</sup>/h) was treated under experimental conditions, and the cost of ClO<sub>2</sub> per day can be calculated by the formula (32). The price of industrial chemicals with a ClO<sub>2</sub> content of 48% was 30 CNY/kg according to the 1688 wholesale platform.

$$\text{Cost}_C = 24 \times 1000 \times 3600 \times \frac{m_{\text{ClO}_2}}{48\%} \times 30 \quad (32)$$

### 2.6.3. The cost-benefit and application analysis

According to the above calculation, the cost of energy and chemicals consumption was calculated by the formula (33):

$$\text{Cost} = \text{Cost}_E + \text{Cost}_C \quad (33)$$

From the perspective of chemicals consumption, the 3.00 bar inlet pressure and 0.30 bar outlet pressure were the best working conditions among the pressure combinations that were studied. From the perspective of energy balance, lower inlet pressure and higher outlet pressure seemed to be beneficial contributed to energy consumption reduction. However, the suction pressure of the gas would be higher with the low inlet pressure or high outlet pressure of the HC reactor (Table 1). The higher suction pressure will cause a higher exhaust back pressure, which may affect the operation of the diesel engine. When energy consumption, ClO<sub>2</sub> consumption, and engine performance were taken into account, the 3.00 bar inlet pressure and the 0.30 bar outlet pressure were reasonable choices.

## 3. Conclusions

We have demonstrated that hydrodynamic cavitation was a valid method for denitrification and significant results were obtained. The HC reactor could induce a large quantity of Gas-Filled-Bubbles. The gas-liquid contact area was greatly expanded, and the chemical reaction rate was significantly enhanced. The gas phase reaction in the Gas-Filled-Bubbles increased the reaction mode of ClO<sub>2</sub> and NO, and thus enhanced the denitration effect. Hydroxyl radicals generated by cavitation promoted the oxidation of NO and microjets improved the gas-liquid mass transfer effect. The HC reactor greatly increased the rate of chemical reactions and resulted in rapid consumption of oxidant in the solution, which was manifested by a rapid decrease after maintaining a particular time of high NO<sub>x</sub> removal rate. The HC reactor enhanced the absorption of NO<sub>2</sub> by the ClO<sub>2</sub> solution, over a range of pH from 4.54 to 5.63. The highest NO<sub>2</sub> concentration of only 20 ppm was found during the hydrodynamic cavitation denitration experiments by use of 1.0 mg/L ClO<sub>2</sub>. The increase in the concentration of ClO<sub>2</sub> significantly prolonged the effective denitrification time, but also led to an increase in the concentration of NO<sub>2</sub>, which indicated there was more escape of ClO<sub>2</sub> at higher concentrations.

The increase of the inlet pressure may either promoted or inhibited the denitration effect. On the one hand, the higher inlet pressure of HC reactor increased the liquid-gas ratio, reduced the size of the bubbles and strengthened the effect of cavitation. On the other, the reaction time decreased as the inlet pressure increased. Moreover, the high-temperature bubbles caused by higher inlet pressures were detrimental to the oxidation of NO by ClO<sub>2</sub>. The outlet pressure of the HC reactor had a similar mechanism to the inlet pressure for hydrodynamic cavitation denitration.

The lower inlet pressure and higher outlet pressure of the HC reactor contributed to energy consumption reduction but affected the denitration efficiency of ClO<sub>2</sub>. However, too low inlet pressure or too high outlet pressure would reduce the suction capacity of the HC reactor, which in turn affected the performance of the diesel engine. When energy consumption, ClO<sub>2</sub> consumption, and engine performance were taken into account, the 3.00 bar inlet pressure and the 0.30 bar outlet pressure were reasonable choices.

## 4. Experimental

### 4.1. Materials

High purity ClO<sub>2</sub> solution (ClO<sub>2</sub>, 830 mg/L, H<sub>2</sub>O) (purity ≥ 99.99%) was purchased from Guangzhou ZLDL Materials Technology Co., Ltd, Guangdong, China. Argon was used as the balance gas in these experiments. Standard gases included NO (900 × 10<sup>-6</sup> mol/mol, balance with Ar) and Argon (purity ≥ 99.999%) which were the products of Dalian Special gases Co. Ltd. Pure water (18.2 MΩcm at 25.0 °C) was obtained from a Milli-Q Plus water purification system (Millipore). The venturi injector (mode 384) was purchased from Mazzei Injector Company, LLC, Bakersfield, USA. Photograph of the bubbles after HC reactor and bubbling reactor were taken by the phantom v2012 high-speed camera with 10,000 fps. The concentration of NO, NO<sub>2</sub> was measured by Madur GA-21 Plus gas analyzer. The pH values were measured by Mettler-Toledo s210 SevenCompact™ pH. The reaction sample was analyzed with Thermo Scientific DIONEX ICS-600 ion chromatography. The liquid flow rate was measured by the turbine flow transducer (LWGY-10, Jinhu Heshi Instrument Co., Ltd., China).

### 4.2. Experimental setup

The experimental setup consisted of a closed-loop reactor comprising low-temperature thermostat bath, HC reactor, Gas distribution system and gas analyzer system (Fig. 8). 10.0 L of ClO<sub>2</sub> solution in the thermostat bath tank was used for recycling. The pump drew the ClO<sub>2</sub> solution from the thermostat bath tank and drove the liquid flow through the line. This valve-controlled experimental device worked either in cavitation treatment mode or bubbling treatment mode.

The cavitation mode was activated when valves 1, 2, 4, 5 and 7 were kept open, and valve 8 was kept closed. The inlet and outlet pressure across the HC reactor were adjusted by tuning valves 1 and 4. High-speed motive flow through the HC reactor created low suction pressure and drew the NO mixture. The NO mixture flow rate was controlled by the Mass flow meter. The gas mixtures entered the liquid, formed Gas-Filled-Bubbles, and then flew across the first stage gas-liquid separator/Bubbling reactor. The Gas-Filled-Bubbles and motive liquid passed the HC reactor together and reached the first stage gas-liquid separator/Bubbling reactor where the liquid level was controlled by valve 5. The treated gas mixture separated in the first stage gas-liquid separator/Bubbling reactor passed the second gas-liquid separator and the gas analyzer in sequence. At the same time, the liquid passed through valve 5 and then returned to the thermostat bath tank.

The bubbling mode was used to make a reference experiment for the cavitation denitration experiment. Having valves 2 and 7 kept closed, the motive flow would directly enter the First stage gas-liquid separator/Bubbling reactor. Having valves 3 and 8 kept open, the NO mixture entered the first stage gas-liquid separator/Bubbling reactor through the valve 4 directly. The liquid level in the gas-liquid separator/Bubbling reactor was retained by adjusting valve 3. The gases reacted with the liquid solution in the Bubbling reactor and was then analyzed by the Madur GA-21 Plus gas analyzer.

### 4.3. Measurement of gas concentration and pH.

Before each experiment, the NO mixture gas was directly introduced into the gas analyzer to determine the initial value. Prior to the experiment, the experimental system was purged by the use of high purity argon until the flue gas analyzer showed an oxygen content of 0%. Then, the NO mixture to be treated was introduced, and the data recording was started. The concentration of NO, NO<sub>2</sub>, and NO<sub>x</sub> was simultaneously recorded with a time interval of 5 s. The pH value was measured in real time, and the data sampling period was synchronized with the flue gas analyzer. The duration of each experiment was 600 s, and 120 sets of data were obtained.

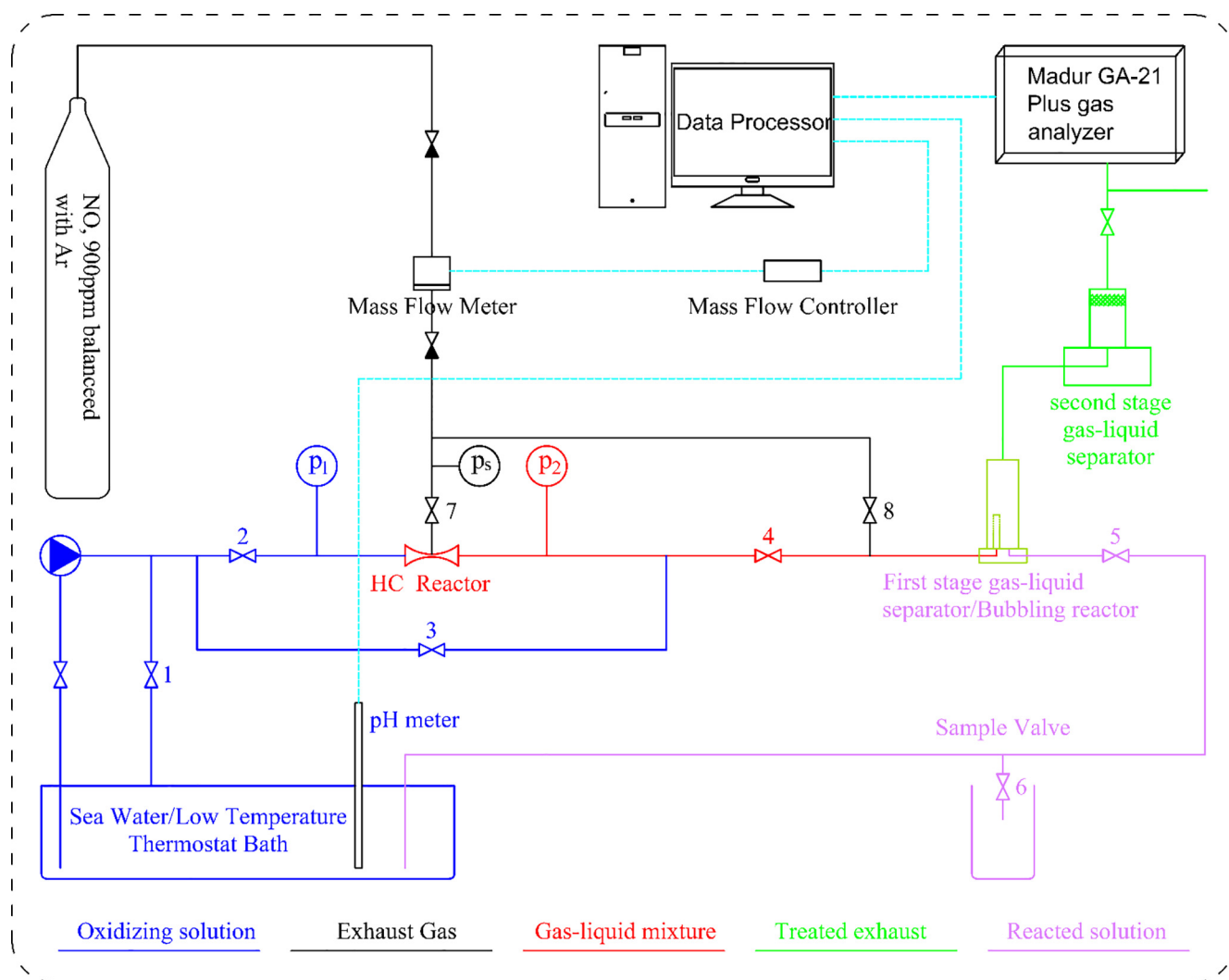


Fig. 8. Experiment schematic diagram.

#### 4.4. Description of bubble size and velocity

Four thousand images were taken continuously by use of the high-speed camera under each working condition with an imaging rate of 10,000 fps and divided into four groups on average. One hundred photos were taken continuously from each set of photos for closer observation. Then, 11 consecutive images with clearly bubble boundaries and motion trajectories were selected.

Photoshop was used to draw a baseline at the same location on the photo, then four corresponding bubbles were identified as the subject of the calculation. Bubbles were measured using FastStone Capture, and the measurements of the four diameters were averaged to obtain the diameter of the bubble. The rising distance was determined by analyzing the trajectory of the bubble and then divided by 0.001 s to get the velocity of the bubble. A theoretical diameter calculation was used to verify the accuracy of the identified method in this study (Supplementary Table S4).

#### 4.5. Detection of ions in reacted solution

A baseline calibration of ion chromatography (ICS-600, Dionex, America) was performed before each test, and standard calibration was performed each month. Before each experiment, a deionized water sample test was performed. On the one hand, the performance of the ion chromatography was checked, and on the other hand, the water

quality was checked to prevent measurement errors due to poor water quality. Took 30.0 mL of the reacted solution and filtered with 0.45  $\mu\text{m}$  IC syringe filters. After that 5 mL of the filtered sample was put into a test tube, which was placed into the autosampler, and the test was started. The test was repeated three times, and the results were recorded accordingly.

#### Author contributions

Liguo Song designed experiments, Jingang Yang, Shubo Yu, Yuanhuang Liang carried out experiments and analyzed data. Minyi Xu provided constructive suggestions on experimental design, paper structure, and text modification. Xinxiang Pan and Li Yao conceived and co-led the project. All authors contributed to the writing of the manuscript. Liguo Song led the initial analysis and coordinated the submission efforts.

#### Conflicts of interest

There are no conflicts to declare.

#### Acknowledgments

The research described in this study was based on work supported by the National Natural Science Foundation of China (51709029,

51779024, 51809100) the Fundamental Research Funds for the Central Universities (3132018257, 3132016337), and the Scientific Research Fund of Liaoning Provincial Education Department of China (20180550574).

Dr. Yang Shaolong, Dr. Yu Yixuan, and Dr. Fu Ke gave great help in the revision of the paper.

## Appendix A. Supplementary data

Supplementary data to this article can be found online at <https://doi.org/10.1016/j.cej.2019.05.094>.

## References

- [1] Regina Asariotis, Mark Assaf, Hassiba Benamara, Marco Fugazza, Jan Hoffmann, Anila Premti, Luisa Rodríguez, Review of Maritime Transport 2017: UNCTAD/RMT/2017, United Nations Publication, 2017.
- [2] E. Harroul-Kolieb, Shipping Impacts on Climate: A Source with Solutions, Oceana, Washington, DC, 2008.
- [3] T.I. IMO, Greenhouse Gas Study 2014, Executive Summary and Final Report.
- [4] Lower emissions on the high seas, *Nature* 551 (2017) 5–6.
- [5] Z. Wan, M. Zhu, S. Chen, D. Sperling, Pollution: three steps to a green shipping industry, *Nature* 530 (2016) 275–277.
- [6] J.G.J. Olivier, K.M. Schure, J. Peters, Trends in Global CO<sub>2</sub> and Total Greenhouse Gas Emissions, (2017).
- [7] N. Olmer, B. Comer, B. Roy, X. Mao, D.A.N. Rutherford, Greenhouse Gas Emissions from Global Shipping 2013–2015, (2017).
- [8] J. van Aardenne, A. Colette, B. Degraeuwe, P. Hammingh, I. de Vlieger, The Impact of International Shipping on European Air Quality and Climate Forcing, (2013).
- [9] A. Aulinger, V. Matthias, M. Zeretzke, J. Bieser, M. Quante, A. Backes, The impact of shipping emissions on air pollution in the greater North Sea region—Part 1: current emissions and concentrations, *Atmos. Chem. Phys.* 16 (2016).
- [10] J.J. Corbett, J.J. Winebrake, E.H. Green, P. Kasibhatla, V. Eyring, A. Lauer, Mortality from ship emissions: a global assessment, *Environ. Sci. Technol.* 41 (2007) 8512–8518.
- [11] M. Sofiev, J.J. Winebrake, L. Johansson, E.W. Carr, M. Prank, J. Soares, J. Vira, R. Kouznetsov, J.-P. Jalkanen, J.J. Corbett, Cleaner fuels for ships provide public health benefits with climate tradeoffs, *Nat. Commun.* 9 (2018) 406.
- [12] S. Aksoyoglu, U. Baltensperger, A.S.H. Prévôt, Contribution of ship emissions to the concentration and deposition of air pollutants in Europe, *Atmos. Chem. Phys.* 16 (2016) 1895–1906.
- [13] B. Claremar, K. Haglund, A. Rutgersson, Ship emissions and the use of current air cleaning technology: contributions to air pollution and acidification in the Baltic Sea, *Earth Syst. Dyn.* 8 (2017) 901.
- [14] R.K. Pachauri, M.R. Allen, V.R. Barros, J. Broome, W. Cramer, R. Christ, J.A. Church, L. Clarke, Q. Dahe, P. Dasgupta, Climate change 2014: synthesis report, Contribution of Working Groups I, II and III to the fifth Assessment Report of the Intergovernmental Panel on Climate Change, IPCC, 2014.
- [15] G. Busca, L. Lietti, G. Ramis, F. Berti, Chemical and mechanistic aspects of the selective catalytic reduction of NO<sub>x</sub> by ammonia over oxide catalysts: a review, *Appl. Catal. B: Environ.* 18 (1998) 1–36.
- [16] T.-W. Chien, H. Chu, Removal of SO<sub>2</sub> and NO from flue gas by wet scrubbing using an aqueous NaClO<sub>2</sub> solution, *J. Hazard. Mater.* 80 (2000) 43–57.
- [17] M.A. Gómez-García, V. Pitchon, A. Kiennemann, Pollution by nitrogen oxides: an approach to NO(x) abatement by using sorbing catalytic materials, *Environ. Int.* 31 (2005) 445–467.
- [18] K. Skalska, J.S. Miller, S. Ledakowicz, Trends in NO<sub>x</sub> abatement: a review, *Sci. Total Environ.* 408 (2010) 3976–3989.
- [19] G.H. Abd-Alla, Using exhaust gas recirculation in internal combustion engines: a review, *Energy Convers. Manage.* 43 (2002) 1027–1042.
- [20] U. Asad, M. Zheng, Exhaust gas recirculation for advanced diesel combustion cycles, *Appl. Energy* 123 (2014) 242–252.
- [21] P.S. Divekar, X. Chen, J. Tjong, M. Zheng, Energy efficiency impact of EGR on organizing clean combustion in diesel engines, *Energy Convers. Manage.* 112 (2016) 369–381.
- [22] L. Feng, J. Tian, W. Long, W. Gong, B. Du, D. Li, L. Chen, Decreasing NO<sub>x</sub> of a low-speed two-stroke marine diesel engine by using in-cylinder emission control measures, *Energies* 9 (2016) 304.
- [23] G. Fontana, E. Galloni, Experimental analysis of a spark-ignition engine using exhaust gas recycle at WOT operation, *Appl. Energy* 87 (2010) 2187–2193.
- [24] D.T. Hountalas, G.C. Mavropoulos, K.B. Binder, Effect of exhaust gas recirculation (EGR) temperature for various EGR rates on heavy duty DI diesel engine performance and emissions, *Energy* 33 (2008) 272–283.
- [25] A. Maiboom, X. Tazua, J.-F. Héret, Experimental study of various effects of exhaust gas recirculation (EGR) on combustion and emissions of an automotive direct injection diesel engine, *Energy* 33 (2008) 22–34.
- [26] S. Verhelst, P. Maesschalck, N. Rombaut, R. Sierens, Increasing the power output of hydrogen internal combustion engines by means of supercharging and exhaust gas recirculation, *Int. J. Hydrogen Energy* 34 (2009) 4406–4412.
- [27] R. Verschaeren, W. Schaeppdryver, T. Serruys, M. Bastiaen, L. Vervaeke, S. Verhelst, Experimental study of NO<sub>x</sub> reduction on a medium speed heavy duty diesel engine by the application of EGR (exhaust gas recirculation) and Miller timing, *Energy* 76 (2014) 614–621.
- [28] M. Zheng, G.T. Reader, J.G. Hawley, Diesel engine exhaust gas recirculation—a review on advanced and novel concepts, *Energy Convers. Manage.* 45 (2004) 883–900.
- [29] C. Deniz, B. Zincir, Environmental and economical assessment of alternative marine fuels, *J. Clean. Prod.* 113 (2016) 438–449.
- [30] O. Schinas, M. Butler, Feasibility and commercial considerations of LNG-fueled ships, *Ocean Eng.* 122 (2016) 84–96.
- [31] F. Burel, R. Taccani, N. Zuliani, Improving sustainability of maritime transport through utilization of Liquefied Natural Gas (LNG) for propulsion, *Energy* 57 (2013) 412–420.
- [32] H.O. Kristensen, Energy demand and exhaust gas emissions of marine engines, *Clean Ship. Curr.* 1 (2012) 18–26.
- [33] M.I. Lamas, C.G. Rodríguez, Emissions from marine engines and NO<sub>x</sub> reduction methods, *J. Maritime Res.* 9 (2012) 77–81.
- [34] G. Qi, R.T. Yang, Low-temperature selective catalytic reduction of NO with NH<sub>3</sub> over iron and manganese oxides supported on titania, *Appl. Catal. B: Environ.* 44 (2003) 217–225.
- [35] V. Jayaram, A. Nigam, W.A. Welch, J.W. Miller, D.R. Cocker III, Effectiveness of emission control technologies for auxiliary engines on ocean-going vessels, *J. Air Waste Manage. Assoc.* 61 (2011) 14–21.
- [36] Y. Zhu, Q. Hou, M. Shreka, L. Yuan, S. Zhou, Y. Feng, C. Xia, Ammonium-salt formation and catalyst deactivation in the SCR system for a marine diesel engine, *Catalysts* 9 (2018).
- [37] H. Thomson, J.J. Corbett, J.J. Winebrake, Natural gas as a marine fuel, *Energy Policy* 87 (2015) 153–167.
- [38] Y.G. Adewuyi, N.Y. Sakyi, M. Arif Khan, Simultaneous removal of NO and SO<sub>2</sub> from flue gas by combined heat and Fe<sup>2+</sup> activated aqueous persulfate solutions, *Chemosphere* 193 (2018) 1216–1225.
- [39] A.H. Hultén, P. Nilsson, M. Samuelsson, S. Ajdari, F. Normann, K. Andersson, First evaluation of a multicomponent flue gas cleaning concept using chlorine dioxide gas – experiments on chemistry and process performance, *Fuel* 210 (2017) 885–891.
- [40] J. Yan, F. Zhou, Y. Zhou, X. Wu, Q. Zhu, H. Liu, H. Lu, Wet oxidation and absorption procedure for NO<sub>x</sub> removal, *Environ. Technol. Innov.* 11 (2018) 41–48.
- [41] R.P. Taleyarkhan, C.D. West, J.S. Cho, R.T. Lahey, R.I. Nigmatulin, R.C. Block, Evidence for nuclear emissions during acoustic cavitation, *Science* 295 (2002) 1868–1873.
- [42] Y.T. Didenko, W.B. McNamara, K.S. Suslick, Hot spot conditions during cavitation in water, *J. Am. Chem. Soc.* 121 (1999) 5817–5818.
- [43] K.S. Suslick, Sonochemistry, *Science* 247 (1990) 1439–1445.
- [44] K.S. Suslick, N.C. Eddingsaas, D.J. Flannigan, S.D. Hopkins, H. Xu, The chemical history of a bubble, *Acc. Chem. Res.* (2018).
- [45] S. You, M.-W. Chen, D.D. Dlott, K.S. Suslick, Ultrasonic hammer produces hot spots in solids, *Nature Commun.* 6 (2015) 6581 EP.
- [46] I. Kim, I. Lee, S.H. Jeon, T. Hwang, J.-I. Han, Hydrodynamic cavitation as a novel pretreatment approach for bioethanol production from reed, *Bioresour. Technol.* 192 (2015) 335–339.
- [47] D. Musmarra, M. Prisciandaro, M. Capocelli, D. Karatza, P. Iovino, S. Canzano, A. Lancia, Degradation of ibuprofen by hydrodynamic cavitation: reaction pathways and effect of operational parameters, *Ultrason. Sonochem.* 29 (2016) 76–83.
- [48] M. Dular, T. Griessler-Bulc, I. Gutierrez-Aguirre, E. Heath, T. Kosjek, A.K. Klemenčič, M. Oder, M. Petkovšek, N. Rački, M. Ravnikar, Use of hydrodynamic cavitation in (waste) water treatment, *Ultrason. Sonochem.* 29 (2016) 577–588.
- [49] L.F. Chuah, S. Yusup, A.R. Abd Aziz, A. Bokhari, M.Z. Abdullah, Cleaner production of methyl ester using waste cooking oil derived from palm olein using a hydrodynamic cavitation reactor, *J. Clean. Prod.* 112 (2016) 4505–4514.
- [50] A.V. Mohod, P.R. Gogate, G. Viel, P. Firmino, R. Giudici, Intensification of biodiesel production using hydrodynamic cavitation based on high speed homogenizer, *Chem. Eng. J.* 316 (2017) 751–757.
- [51] A.G. Chakinala, P.R. Gogate, A.E. Burgess, D.H. Bremner, Treatment of industrial wastewater effluents using hydrodynamic cavitation and the advanced Fenton process, *Ultrason. Sonochem.* 15 (2008) 49–54.
- [52] Amrutlal L. Prajapat, Parag R. Gogate, Intensified depolymerization of aqueous polyacrylamide solution using combined processes based on hydrodynamic cavitation, ozone, ultraviolet light and hydrogen peroxide, *Ultrason. Sonochem.* 31 (2016) 371–382.
- [53] Jian Long Wang, Xu Le Jin, Advanced oxidation processes for wastewater treatment: formation of hydroxyl radical and application, *Crit. Rev. Environ. Sci. Technol.* 42 (2012) 251–325.
- [54] Pankaj Chowdhury, T. Viraraghavan, Sonochemical degradation of chlorinated organic compounds, phenolic compounds and organic dyes – a review, *Sci. Total Environ.* 407 (2009) 2474–2492.
- [55] Arnim Henglein, Chemical effects of continuous and pulsed ultrasound in aqueous solutions, *Ultrason. Sonochem.* 2 (1995) S115–S121.
- [56] Y.G. Adewuyi, Sonochemistry: environmental science and engineering applications, *Ind. Eng. Chem. Res.* 40 (2001) 4681–4715.
- [57] Masahiro Kohno, Takayuki Mukudai, Toshihiko Ozawa, Yoshimi Niwano, Free radical formation from sonolysis of water in the presence of different gases, *J. Clin. Biochem. Nutr.* 49 (2011) 96–101.
- [58] M. Gutierrez, A. Henglein, J.K. Dohrmann, Hydrogen atom reactions in the sonolysis of aqueous solutions, *J. Phys. Chem.* 91 (1987) 6687–6690.
- [59] L. Dharmarathne, M. Ashokkumar, F. Grieser, On the generation of the hydrated electron during the sonolysis of aqueous solutions, *J. Phys. Chem. A* 117 (2013)

- 2409–2414.
- [60] A. Moghimi, Separation and extraction of Co(II) using magnetic chitosan nanoparticles grafted with beta-cyclodextrin and determination by FAAS, Russian J. Phys. Chem. A 88 (2014) 2157–2164.
- [61] Y. Zhao, T.-X. Guo, Z.-Y. Chen, Y.-R. Du, Simultaneous removal of SO<sub>2</sub> and NO using M/NaClO<sub>2</sub> complex absorbent, Chem. Eng. J. 160 (2010) 42–47.
- [62] C. Brogren, H.T. Karlsson, I. Bjerle, Absorption of NO in an aqueous solution of NaClO<sub>2</sub>, Chem. Eng. Technol. Ind. Chem.-Plant Equip.-Process Eng. Biotechnol. 21 (1998) 61–70.
- [63] B.R. Deshwal, S.H. Lee, J.H. Jung, B.H. Shon, H.K. Lee, Study on the removal of NO<sub>x</sub> from simulated flue gas using acidic NaClO<sub>2</sub> solution, J. Environ. Sci. 20 (2008) 33–38.
- [64] N.D. Hutson, R. Krzyzyska, R.K. Srivastava, Simultaneous removal of SO<sub>2</sub>, NO<sub>x</sub>, and Hg from coal flue gas using a NaClO<sub>2</sub>-enhanced wet scrubber, Ind. Eng. Chem. Res. 47 (2008) 5825–5831.
- [65] R. Krzyzyska, N.D. Hutson, Effect of solution pH on SO<sub>2</sub>, NO<sub>x</sub>, and Hg removal from simulated coal combustion flue gas in an oxidant-enhanced wet scrubber, J. Air Waste Manage. Assoc. 62 (2012) 212–220.
- [66] B.R. Deshwal, D.S. Jin, S.H. Lee, S.H. Moon, J.H. Jung, H.K. Lee, Removal of NO from flue gas by aqueous chlorine-dioxide scrubbing solution in a lab-scale bubbling reactor, J. Hazard. Mater. 150 (2008) 649–655.
- [67] D.-S. Jin, B.-R. Deshwal, Y.-S. Park, H.-K. Lee, Simultaneous removal of SO<sub>2</sub> and NO by wet scrubbing using aqueous chlorine dioxide solution, J. Hazard. Mater. 135 (2006) 412–417.
- [68] Z. Han, S. Yang, D. Zheng, X. Pan, Z. Yan, An investigation on NO removal by wet scrubbing using NaClO<sub>2</sub> seawater solution, SpringerPlus 5 (2016) 751.
- [69] P.S. Kumar, A.B. Pandit, Modeling hydrodynamic cavitation, Chem. Eng. Technol. Ind. Chem.-Plant Equip.-Process Eng.-Biotechnol. 22 (1999) 1017–1027.
- [70] P. Senthil Kumar, M. Siva Kumar, A.B. Pandit, Experimental quantification of chemical effects of hydrodynamic cavitation, Chem. Eng. Sci. 55 (2000) 1633–1639.
- [71] H. Vogt, J. Balej, J.E. Bennett, P. Wintzer, S.A. Sheikh, P. Gallone, S. Vasudevan, K. Pelin, Chlorine oxides and chlorine oxygen acids, Ullmann's Encyclopedia of Industrial, Chemistry (2000).
- [72] A.K. Horváth, I. Nagypál, G. Peintler, I.R. Epstein, Autocatalysis and self-inhibition: coupled kinetic phenomena in the chlorite – tetrathionate reaction, J. Am. Chem. Soc. 126 (2004) 6246–6247.
- [73] A.K. Horváth, I. Nagypál, I.R. Epstein, Three autocatalysts and self-inhibition in a single reaction: a detailed mechanism of the chlorite – tetrathionate reaction, Inorgan. Chem. 45 (2006) 9877–9883.